Enhancement of Rotator Cuff Tendon-bone Healing with Graphene Oxide/PRP Composite Scaffold in a Rabbit Model: A Histological and Biomechanical Study

Bo Qin
Affiliated Traditional Chinese Medicine Hospital of Southwest Medical University
https://orcid.org/0000-0002-4283-4041
Dingsu Bao
Affiliated Traditional Chinese Medicine Hospital of Southwest Medical University
Shengqiang Zeng
Affiliated Traditional Chinese Medicine Hospital of Southwest Medical University
Kai Deng
Affiliated Traditional Chinese Medicine Hospital of Southwest Medical University
Gang Liu
Affiliated Traditional Chinese Medicine Hospital of Southwest Medical University
Zhengrong Xiong
Affiliated Traditional Chinese Medicine Hospital of Southwest Medical University
Min Gong
Chengdu University of Traditional Chinese Medicine Affiliated Hospital
Siyuan He
Southern Medical University
Jie Shi
Affiliated Traditional Chinese Medicine Hospital of Southwest Medical University
Xun Wang
Affiliated Traditional Chinese Medicine Hospital of Southwest Medical University
Zhiqiang Lu
Affiliated Traditional Chinese Medicine Hospital of Southwest Medical University
Shijie Fu (fushijieggj@126.com)
Affiliated Traditional Chinese Medicine Hospital of Southwest Medical University
https://orcid.org/0000-0002-2168-6094

Research article

Keywords: Platelet-rich plasma, Graphene oxide, Rotator cuff tear, Tendon-bone healing

Posted Date: December 1st, 2020

DOI: https://doi.org/10.21203/rs.3.rs-116150/v1

Abstract

Background: Application of platelet-rich plasma (PRP) can improve tendon-bone healing (TBH) after rotator cuff surgical repair. Graphene Oxide (GO) is a steady, controlled, and sustained carrier. The purpose of this study is to determine whether GO/PRP Composite Scaffold enhances the TBH after RC surgical repair in a rabbit model.

Methods: A full-thickness tear of the supraspinatus tendon was created and repaired in 36 adult male New Zealand rabbits. They were divided into three groups: Control group, PRP group, and GO/PRP Composite Scaffold group (GO group). The effect of GO/PRP Composite Scaffold on TBH was assessed using histological and biomechanical evaluations at 8 and 12 weeks postoperatively.

Results: Histological analysis showed that greater continuity, better orientation, and more density of collagen fiber were detected in the GO group than PRP and Control groups at 8 and 12 weeks, respectively. Results of biomechanical evaluations showed that the load to failure and stiffness of the GO group were statistically higher than those of PRP and Control groups at both 8 and 12 weeks ($P<0.05$). Compared with 8 weeks in the GO group, there was no significant difference in load to failure at 12 weeks ($P>0.05$), while the stiffness at 12 weeks was higher than that at 8 weeks ($P<0.05$).

Conclusions: These results demonstrated that GO/PRP Composite Scaffold enhanced the TBH following rotator cuff surgical repair in a rabbit model. The GO may be an effective carrier for PRP into repair sites.

Background

Rotator cuff tear (RCT) is a common and frequent injury in sports medicine, with figures ranging from 20 to 54% in those aged from 60 to 80 years [1, 2]. Surgical repair of RCT is one of the most commonly performed procedures because of its positive outcomes. However, previous studies have reported high re-tear rates following RC repair, accounting for 26–94% [3–5]. The re-tear of RC repair negatively affects long-term clinical outcomes. Tendon-bone healing (TBH) is vital to the ultimate success. Facilitate the quality of TBH is the core of repair and functional rehabilitation [4]. Therefore, new biologic strategies that enhance the TBH response are subjects of interest in sports medicine [4–7].

Recently, Platelet-rich plasma (PRP) is the most studied intervention and can enhance TBH [6–8]. PRP is a type of whole blood concentrate that is obtained through centrifugation [9]. It is an autologous source of various growth factors, including transforming growth factor (TGF), platelet-derived growth factor (PDGF), vascular endothelial growth factor (VEGF), insulin-like growth factor (IGF), epidermal growth factor (EGF), and so on [6, 9, 10]. TBH is the result of various growth factors. The above growth factors are stored in PRP and play a role in TBH's surgical repair [6]. Current literature [10, 11] has confirmed that PRP is a promising way to accelerate the TBH process and augment tissues with low healing ability. However, though PRP can act as a carrier of the above factors, the effect may be transient due to its functional half-life, rapid dispersal, and poor stability in vivo [7, 12]. Jensen and Shin [13] proposed that PRP alone without any carrier could not improve bone regeneration and may not effectively enhance

healing. This may be related to the relatively short time that PRP stays tendon-bone interface (TBI). Thus, a long-term and stable carrier is needed for the slow and unsustainable release of PRP's various growth factors in the repair site.

Currently, graphene, the thinnest nanomaterial, has attracted much interest and has been widely used in tissue engineering [14]. Graphene oxide (GO) is a derivative of graphene with a typical quasi-two-dimensional spatial structure [14, 15]. GO has been widely applied as a carrier for drugs and other biomolecules and controlled release since Shen's first work in 2010[16, 17]. Subsequent investigators [16, 18, 19] have reported that GO can provide high mechanical strength and has osteogenic and chondrogenic induction capability, promoting the proliferation, differentiation, and adhesion of cultured cells. On the other hand, GO is anti-bacterial, anti-inflammatory, mineralizable with apatite, and non-toxic to human osteoblast [20]. Taken together, the findings from these investigations suggest that GO is a biocompatible, biodegradable, and biomimetic carrier with good mechanical properties and dispersion stability [21, 22]. Hence, we hypothesized that GO could be a stable and effective carrier to deliver and localize PRP's various growth factors to the repair site.

This study aimed to determine whether the application of GO/PRP Composite Scaffold facilitates TBH after RC surgical repair in a rabbit model.

Methods

Study design

All the procedures were approved by the Ethical Inspection Committee at Southwest Medical University (No. 2020680) and performed according to the internationally accredited guidelines. 36 adult male New Zealand rabbits (age, 12–14 weeks; body weight, 4.0 ± 0.5 kg) were used in this study. All the rabbits were provided by the experiment animal center of Southwest Medical University (Production license number: SCXK[Chuan]2018-17; the use license number: SYXK[Chuan]2018-065). All the rabbits were reared in the cage separately (Cage: 65*45*40 cm), taking a rabbit diet and drink freely.

Surgical Procedures

The 36 adult male New Zealand rabbits treated with acute full-thickness RCT were divided into the following three groups: Control group, PRP group, and GO/PRP Composite Scaffold group (GO group). The allocation of rabbits was shown (Fig. 1).

Rabbits were anesthetized successfully. Both legs were shaved and aseptically prepared for surgery. A 2-cm longitudinal skin incision was made. A dissection was made on the deltoid muscle to expose the supraspinatus tendon. A full-thickness supraspinatus tendon tear was made by cutting the tendon from the greater tuberosity's footprint.

After the full-thickness RCT was prepared, the free end of the torn supraspinatus tendon was repaired in mattress suture with 2 – 0 absorbable sutures (NO.2 Ethibond, Ethicon Inc, Somerville, NJ, USA). Two

parallel bone tunnels were established at the footprints of greater tuberosity with a syringe needle. Then, the PDS suture was passed through the tunnels. The 2 − 0 absorbable sutures on the same side of the tunnel were pulled out with PDS suture as a lead wire. The 0 absorbable sutures (NO.0 Ethibond, Ethicon Inc, Somerville, NJ, USA) were tied with the end of the 2 − 0 sutures. The 0 sutures were then pulled out with 2 − 0 sutures as a lead wire again. Lastly, the 0 sutures which were pulled out from the bone tunnels were fastened and fixed. The incision was closed with sutures (Fig. 2).

Control group: the RCT models were created and repaired without any interventions. PRP group: the PRP was immediately pipetted onto the repair site intra-operatively. GO group: GO/PRP Composite Scaffold was immediately pipetted onto the repair site intra-operatively. A total of 0.5 mL of the corresponding scaffold was injected into the repair site in each rabbit.

Platelet-Rich Plasma Preparation

The preparation of PRP was used by twice centrifugation (Landesberg method). Under anesthesia before surgical procedures, 9 mL autologous blood was acquired from the central auricular artery in each rabbit. 1 mL of 10% sodium citrate was immediately added to the blood sample as an anticoagulant. The blood was processed and stored at 4℃. The whole blood sample was centrifuged at 1200 rpm for 10 min to separate the plasma containing the platelets from the inferior layer's red blood cells. The platelet-rich layer was centrifuged at 1200 rpm for 15 min to obtain a cell pellet within the supernatant. After removing the platelet-poor plasma, PRP was aspirated with a pipette and placed in a sterile tube. The amount of PRP was approximately 1 mL.

The PRP gel: 1 mL PRP mixed with 80 u/mL thrombin for activation was used within minutes to add to the rotator cuff repair site.

GO/PRP Composite Scaffold Preparation

The GO is purchased and obtained from the company (TNGO-50, Chengdu Organic Chemicals Co. Ltd., Chinese Academy of Sciences, China). In line with previous reports, 1.5 mg GO was suspended in 1 mL distilled water, and the mixture was sonicated well for 30 min to get the GO dispersion solution. Subsequently, the prepared 2 mL PRP and the GO dispersion solution were mixed in the ratio of 2:1 to get the 0.5 mg/mL mixed solution. After that, the 80 u/mL thrombin was added to the solution, and then the mixture was exposed under UV light for 4 min to form a GO/PRP composite scaffold.

Histologic Evaluation

The greater tuberosity of the humerus and supraspinatus tendon was harvested. The specimens were soaked in neutral buffered 10% formalin solution and fixed for 48 hours before routine processing. The specimens were then decalcified in 10% formic acid, dehydrated with graded alcohol, and cleared in Xylene. They were embedded in a paraffin block and cut into 5 um longitudinal sections. The sections included the greater tuberosity of humerus and supraspinatus tendon and muscle. After staining with hematoxylin-eosin (H&E), a histologic evaluation was performed. The histologic grading system on the

TBH was analyzed semi-quantitatively according to the continuity, orientation, and density of the collagen fiber and the TBI structure's maturation.

Biomechanical Evaluation

The biomechanical testing was conducted at the Biomechanics Laboratory, Affiliated Hospital of Southwest Medical University. The tendon-bone complex was texted using a custom fixture clamping system, an Instron material testing machine (E3000 Linear-Torsion Dynamic Test Instrument).

The tendon-bone complex was harvested at 8 and 12 weeks after the operation. To determine TBI's tensile properties, all surround tissues, except for the supraspinatus tendon, were dissected from a part of the scapula and the humerus. The humeral shaft was transected 4 cm distal to the surgical neck. The supraspinatus tendon was cut 2 cm distal to the footprint of the supraspinatus tendon. Then, the humerus side was secured into the mold with polymethyl methacrylate. The tendon side was wrap with gauze, weave suture, and fasten with glue to prevent slippage. After preloading to 5 N, each specimen was loaded to failure in the tendon in line with the humerus's long axis at a rate of 0.5 mm/min. The ultimate load to failure and failure sites were recorded. Biomechanical stiffness is defined as the length of tissue deformation for a given stress. All tests were carried out at room temperature, and the specimens were kept moist with a normal saline solution during the tests (Fig. 3).

Statistical Analysis

Statistical analysis was carried out using GraphPad Prism software (version 8.0.2) and IBM SPSS software (version 24.0, SPSS Inc, Chicago, IL). All measurements were presented by the mean and standard deviation ($\bar{x} \pm s$). The homogeneity of variance was performed by using the Shapiro-Wilk test. Two-way ANOVA performed the statistical analysis. The Kruskal-Wallis test performed the semiquantitative grades of histological evaluations. A P-value < 0.05 was regarded as statistically significant.

Results

Histological Observations

The histological characteristics were observed at the repair site of TBI among Control, PRP, and GO groups at 8 and 12 weeks after surgery, respectively. (Table 1; Fig. 4). The results were described in Table 1. At 8 and 12 weeks, the GO group showed greater continuity, better orientation, and more collagen fiber density than the Control and PRP groups. There was a significant difference in the TBI structure's maturation between three groups at 8 and 12 weeks, respectively.

Table 1

Results of semiquantitative histological evaluations at 8 and 12 weeks [α]

	Control group				PRP group				GO group			
	G0	G1	G2	G3	G0	G1	G2	G3	G0	G1	G2	G3
8 weeks evaluation												
Continuity	2	4	0	0	1	3	2	0	0	0	4	2
Orientation	1	4	1	0	0	2	3	1	0	0	3	3
Density	1	5	0	0	0	2	3	1	0	0	4	2
Maturation of TBI structure	1	5	0	0	0	3	3	0	0	0	3	3
12 weeks evaluation												
Continuity	0	3	3	0	0	1	3	2	0	0	1	5
Orientation	0	3	3	0	0	0	2	4	0	0	1	5
Density	0	2	4	0	0	0	3	3	0	0	1	5
Maturation of TBI structure	0	2	3	1	0	1	3	2	0	0	0	6

Note: [α] G, grades. Grades were as follows: G1, absent or minimal (< 25% of proportion); G1, mild degree (25%-50%); G2, moderate degree (> 50%-75%); G3, marked degree (> 75%). Control group, repair; PRP group, repair + PRP; GO group, repair + PRP/GO.

At 8 weeks, the TBI of the GO group was composed of well-organized and densely-arranged collagen fibers, regularly arranged chondrocytes, and more Sharpey's fibers with new bone growth into TBI. More densely and better-oriented collagen fibers were observed in the PRP group with some chondrocytes and Sharpey's fibers. However, there were coarse collagen fibers with irregular continuity, fewer chondrocytes, and Sharpey's fibers in the Control group.

At 12 weeks, the GO group showed better collagen fiber continuity, densely organized Sharpey's fibers bridged the TBI and more regular chondrocytes. The continuous and calcified fibrocartilage had replaced the TBI. In the PRP group, densely organized, oriented collagen fibers and Sharpey's fibers were observed vertical to the TBI with new bone growth into TBI, which were better than the Control group. Compared with PRP and GO groups, the Control group showed less arranged collagen fibers and less densely Sharpey's fibers.

Biomechanical Results

The biomechanical tests were conducted among Control, PRP, and GO groups at 8 and 12 weeks after surgery, respectively (Fig. 5). At 8 weeks, the load to failure of the GO group (187.00 ± 13.09 N) and

stiffness (17.98 ± 2.47 N/mm) was the highest compared with PRP and Control groups ($P < 0.05$). The load to failure of the PRP group (155.21 ± 6.32 N) was higher than the Control group ($P < 0.05$). At 12 weeks, the load to failure of the GO group (199.28 ± 27.31 N) and stiffness (29.90 ± 4.56 N/mm) was the highest compared with the PRP and Control groups ($P < 0.05$). The load to failure of the PRP group (159.67 ± 16.00 N) was higher than the Control group ($P < 0.05$). There were no significant between 8 and 12 weeks about load to failure in the GO group ($P > 0.05$). The stiffness at 8 weeks is lower than that at 12 weeks ($P < 0.05$). On the other hand, at 8 weeks, 2 failure cases occurred at the TBI in Control and PRP groups, and 16 cases occurred at the tendinous part of the supraspinatus. At 12 weeks, all failure occurred at the tendinous part of the supraspinatus, not the TBI.

Discussion

Histological and biomechanical results showed that the GO group was better than other groups. This study demonstrated a tissue engineering strategy based on a GO/PRP Composite Scaffold enhanced TBH after RC surgical repair in a rabbit model. The Graphene Oxide may be an effective carrier for PRP into repair sites.

The TBI has a special orderly structure and specific function, consisting of four distinct zones: tendon fiber, unmineralized fibrocartilage, mineralized fibrocartilage, and bone [23]. Direction and indirection insertions are the two types of insertions of TBI [24, 25]. The former contains the above zones in the transition from tendon to bone, while the latter includes the bone, Sharpey's fibers, and ligament. Direct fibrocartilage fixation and indirect Sharpey's fiber of TBI provide different strengths and interface properties. TBH is a process based on cell renewal and differentiation, particularly in bone and cartilage differentiation. The histological analyses in a rabbit model revealed that the positive effect might be caused by GO/PRP composite scaffold on the TBH. As time went on, the TBI went through the process from the growth of granulation to the disappearance, the irregular orientation of collagen fibers to well arrangement of that in a direction parallel to the forced direction, and the increased numbers of chondrocytes and fibrocartilages. At 8 and 12 weeks, the GO group showed greater continuity, better orientation, and more collagen fiber density than other groups ($P < 0.05$). At 12 weeks, the TBI structure maturation in the GO group with a well-organized fibrocartilage transition zone was better than in other groups ($P < 0.05$).

Reviewing the article, there were also other biomaterials used to enhance TBH. Due to the functional half-life and rapid dispersal in vivo, various growth factors released from PRP induces more scar tissue formation on the TBI, thus not improving the mechanical properties of the regenerated tissue [7, 26]. Therefore, controlled and sustained release is required [5]. Zhang [27] found that gelatin sponge as a scaffold to control bioactive factors' release may be useful, and gelatin sponge loading with PRP could prolong PRP's bioactivity time and promote the early TBH in a rabbit model. Gabrielle [12] revealed that freeze-dried chitosan combined with PRP was safe and effective in improving RCT repair in a small animal model. The implant could improve attachment of TBI through increased bone remodeling and inhibited heterotopic ossification. Recently, GO has been performed to test the effect on tissue

engineering and regenerated medicine fields. Shen [28] developed a GO incorporated PDLLA hybrid hydrogel for localized TGF-β3 delivery and sustained release. The scaffold supported TGF-β3 retention for up to 4 weeks and enhanced scaffold compressive stiffness because of GO. Qi [29] also revealed that a sericin/GO composite scaffold, with good biocompatibility, cell adhesive property, proliferation- and migration-promoting effects, and osteogenic property, can effectively promote new bone regeneration and achieve structural and functional repair. The ideal characteristics make GO suitable for being used as a new carrier material.

In the biomechanical evaluations, the results showed some significance at 8 and 12 weeks after surgery. In the TBH process, tendon regeneration, osteoinduction, and chondrogenic-induction are associated with TBH's quality [30]. Consistent with previous literature about PRP [27, 31, 32], we found the load to failure of GO and PRP groups were both higher than the Control group at 8 and 12 weeks ($P < 0.05$), indicating that the application of PRP did improve the biomechanical strength of the repair sites. However, the GO group's load was higher than PRP and Control groups, whether at 8 or 12 weeks ($P < 0.05$), while there was no statistical significance in the load to failure of the GO group between 8 and 12 weeks ($P > 0.05$). These meant that the effect of GO/PRP Composite Scaffold implanted at repair sites was superior to PRP alone in improving the biomechanical properties and promoting TBH. The load to TBI failure may reach the maximum at 8 weeks, consistent with Chung's study [32]. On the other hand, a higher stiffness indicates that the ability to withstand greater stress with the same deformation is beneficial after TBH [33]. The stiffness of the GO group was higher than the PRP and Control groups at 8 and 12 weeks ($P < 0.05$). The interface matures with time, and the stiffness of the GO group is increasing at 8 and 12 weeks ($P < 0.05$), while there was no difference between PRP and Control groups ($P > 0.05$). Recently, several studies [26, 31, 34, 35] demonstrated that the application of fresh PRP alone could improve the integrity of repair sites, but the enhancement of biomechanical properties remained controversial, and even no demonstrable effect. This study used GO for the steady, controlled, and sustained release of PRP's various growth factors. Once the injury of chondrocytes is formed after RCT, they are difficult to regenerate spontaneously. Instead, the fibrocartilage will generate, whose mechanical properties are far less than normal hyaline cartilage [36]. GO/PRP Composite Scaffold could enhance TBH's quality, improve the biomechanical strength and stiffness, restoring the biomechanical properties. This is in line with Wang's and Zhou's researches [20, 37] that GO, as a carrier, possesses good osteogenic, chondrogenic, and angiogenic induction capabilities. The number of Sharpey's fibers determines the tensile strength of the TBI. Consistently, the histological and biomechanical results indicated that compared with 8 weeks in PRP and Control groups, GO/PRP Composite Scaffold could increase the number of Sharpey's fibers, resulting in a higher tensile strength at 12 weeks. In this study, all failures occurred at the tendinous part of the tendon-bone complex, not the TBI at 12 weeks, while failures occurred at 8 weeks. That means that TBH may accomplish in all specimens at 12 weeks after surgery, consistent with Suh's study [38]. The above data support the beneficial effect of GO/PRP Composite Scaffold on the TBH in a rabbit model.

In this study, the advantages of GO/PRP Composite Scaffold are as follows. First, the PRP, containing various growth factors, has a significant curative effect on the TBH, which has been proved. Next, GO is a

steady, controlled, and sustained-release carrier, which enhances TBH by controlling and increasing the release of growth factors into the repair sites. The properties of GO can increase residence time and bioactivity of growth factors of PRP. On the other hand, some important studies have confirmed that the related GO scaffolds show excellently biocompatible, biodegradable, biomimetic, biomechanical properties, large specific surface area, and dispersion stability. GO can make up for the deficiency of PRP and make full use of it. Lastly, GO/PRP Composite Scaffold serves as a 3D bioactive material, positively affecting the TBH. The 3D porous network scaffold, an ideal environment in tissue engineering, can enhance cell numbers and viability, increase osteogenic and chondrogenic differentiation and biological structure plasticity compared with a 2D scaffold. This scaffold can improve healing and mechanical properties at the TBI.

There still exist some limitations. First, the sample size was relatively limited. However, most differences were significant. Secondly, the acute full-thickness RCT model and repair procedure in a rabbit model is different from those in human, limiting the generation of the results. Most RCTs are chronic and degenerative tears in nature. Lastly, the effect was assessed using histological and biomechanical evaluations. GO is a controlled and sustained release. However, the mechanism by which GO/PRP Composite Scaffold induces TBH has not to be further explored, such as specific growth factors, the targets, and signaling pathways.

Conclusions

In this study, the results demonstrated that the GO/PRP Composite Scaffold enhanced the TBH at the TBI in a rabbit model. The GO may be an effective PRP carrier into repair sites, indicating its potential for tissue engineering application.

Abbreviation

RCT: Rotator cuff tear; TBH: Tendon-bone healing; PRP: Platelet-rich plasma; TBI: Tendon-bone interface; GO: Graphene oxide.

Declarations

Acknowledgments

Not applicable.

Funding

This study was supported by the Luzhou Municipal People's Government-Southwest Medical University Science and Technology Cooperation Achievements Transformation Project (2019LZXNYDJ20C01) and Southwest Medical University Scientific and Technological Achievements Transformation Project (0903-00050003).

Availability of data and materials

All data generated or analysed during this study are included in this published article and its supplementary information files.

Author's contributions

QB conducted the researches, wrote and revised the draft manuscript, and subsequent manuscript. BDS designed the study, revised the draft manuscript, and conducted the researches. ZSQ and DK established the animals' model and conducted the animals' surgery. LG designed the study, participated in writing the draft manuscript. XZR, GM, HSY were contributing to the literature search, statistical analysis. SJ, WX, and LZQ performed the histological evaluations and biomechanical evaluations. FSJ contributed the funds collection, and study design. All authors read and approved the final manuscript.

Ethics approval and consent to participate

All the procedures were approved by the Ethical Inspection Committee at Southwest Medical University (No. 2020680) and performed according to the internationally accredited guidelines.

Consent for publication

Not applicable.

Competing interests

The authors declare that they have no competing interests.

References

1. Piper CC, AJ Hughes, Y Ma, H Wang, AS Neviaser. Operative versus nonoperative treatment for the management of full-thickness rotator cuff tears: a systematic review and meta-analysis. J Shoulder Elbow Surg, 2018; 27: 572-76.
2. Kukkonen J, A Joukainen, J Lehtinen, KT Mattila, EK Tuominen, T Kauko, et al:. Treatment of Nontraumatic Rotator Cuff Tears: A Randomized Controlled Trial with Two Years of Clinical and Imaging Follow-up. J Bone Joint Surg Am, 2015; 97: 1729-37.
3. Colvin AC, N Egorova, AK Harrison, A Moskowitz, EL Flatow. National trends in rotator cuff repair. J Bone Joint Surg Am, 2012; 94: 227-33.
4. Zumstein MA, A Lädermann, S Raniga, MO Schär. The biology of rotator cuff healing. Orthop Traumatol Surg Res, 2017; 103: S1-s10.
5. Kim SY, SW Chae, J Lee. Effect of Poloxamer 407 as a carrier vehicle on rotator cuff healing in a rat model. J Orthop Surg Res, 2014; 9: 12.

6. Deprés-Tremblay G, A Chevrier, M Snow, MB Hurtig, S Rodeo, MD Buschmann. Rotator cuff repair: a review of surgical techniques, animal models, and new technologies under development. J Shoulder Elbow Surg, 2016; 25: 2078-85.
7. Lu D, C Yang, Z Zhang, M Xiao. Enhanced tendon-bone healing with acidic fibroblast growth factor delivered in collagen in a rabbit anterior cruciate ligament reconstruction model. J Orthop Surg Res, 2018; 13: 301.
8. Scully D, KM Naseem, A Matsakas. Platelet biology in regenerative medicine of skeletal muscle. Acta Physiol (Oxf), 2018; 223: e13071.
9. Santos S, E Sigurjonsson Ó, CA Custódio, J Mano. Blood Plasma Derivatives for Tissue Engineering and Regenerative Medicine Therapies. Tissue Eng Part B Rev, 2018; 24: 454-62.
10. Pauly S, F Klatte-Schulz, K Stahnke, M Scheibel, B Wildemann. The effect of autologous platelet rich plasma on tenocytes of the human rotator cuff. BMC Musculoskelet Disord, 2018; 19: 422.
11. Wang C, M Xu, W Guo, Y Wang, S Zhao, L Zhong. Clinical efficacy and safety of platelet-rich plasma in arthroscopic full-thickness rotator cuff repair: A meta-analysis. PLoS One, 2019; 14: e0220392.
12. Deprés-Tremblay G, A Chevrier, M Snow, S Rodeo, MD Buschmann. Freeze-dried chitosan-platelet-rich plasma implants improve supraspinatus tendon attachment in a transosseous rotator cuff repair model in the rabbit. J Biomater Appl, 2019; 33: 792-807.
13. Jensen TB, O Rahbek, S Overgaard, K Søballe. Platelet rich plasma and fresh frozen bone allograft as enhancement of implant fixation. An experimental study in dogs. J Orthop Res, 2004; 22: 653-8.
14. Dinescu S, M Ionita, SR Ignat, M Costache, A Hermenean. Graphene Oxide Enhances Chitosan-Based 3D Scaffold Properties for Bone Tissue Engineering. Int J Mol Sci, 2019; 20:
15. Willcox JA, HJ Kim. Molecular Dynamics Study of Water Flow across Multiple Layers of Pristine, Oxidized, and Mixed Regions of Graphene Oxide. ACS Nano, 2017; 11: 2187-93.
16. Kanayama I, H Miyaji, H Takita, E Nishida, M Tsuji, B Fugetsu, et al:. Comparative study of bioactivity of collagen scaffolds coated with graphene oxide and reduced graphene oxide. Int J Nanomedicine, 2014; 9: 3363-73.
17. Shen H, M Liu, H He, L Zhang, J Huang, Y Chong, et al:. PEGylated graphene oxide-mediated protein delivery for cell function regulation. ACS Appl Mater Interfaces, 2012; 4: 6317-23.
18. Belaid H, S Nagarajan, C Teyssier, C Barou, J Barés, S Balme, et al:. Development of new biocompatible 3D printed graphene oxide-based scaffolds. Mater Sci Eng C Mater Biol Appl, 2020; 110: 110595.
19. Liao J, Y Qu, B Chu, X Zhang, Z Qian. Biodegradable CSMA/PECA/Graphene Porous Hybrid Scaffold for Cartilage Tissue Engineering. Sci Rep, 2015; 5: 9879.
20. Wang Q, Y Chu, J He, W Shao, Y Zhou, K Qi, et al:. A graded graphene oxide-hydroxyapatite/silk fibroin biomimetic scaffold for bone tissue engineering. Mater Sci Eng C Mater Biol Appl, 2017; 80: 232-42.

21. Wu J, A Zheng, Y Liu, D Jiao, D Zeng, X Wang, et al:. Enhanced bone regeneration of the silk fibroin electrospun scaffolds through the modification of the graphene oxide functionalized by BMP-2 peptide. Int J Nanomedicine, 2019; 14: 733-51.
22. Mondal MK, S Mukherjee, SK Saha, P Chowdhury, SP Sinha Babu. Design and synthesis of reduced graphene oxide based supramolecular scaffold: A benign microbial resistant network for enzyme immobilization and cell growth. Mater Sci Eng C Mater Biol Appl, 2017; 75: 1168-77.
23. Lu H, F Liu, C Chen, Z Wang, H Chen, J Qu, et al:. Low-Intensity Pulsed Ultrasound Stimulation for Tendon-Bone Healing: A Dose-Dependent Study. Am J Phys Med Rehabil, 2018; 97: 270-77.
24. Teng C, C Zhou, D Xu, F Bi. Combination of platelet-rich plasma and bone marrow mesenchymal stem cells enhances tendon-bone healing in a rabbit model of anterior cruciate ligament reconstruction. J Orthop Surg Res, 2016; 11: 96.
25. Nakase J, K Kitaoka, K Matsumoto, K Tomita. Facilitated tendon-bone healing by local delivery of recombinant hepatocyte growth factor in rabbits. Arthroscopy, 2010; 26: 84-90.
26. Zheng C, H Lu, Y Tang, Z Wang, H Ma, H Li, et al:. Autologous Freeze-Dried, Platelet-Rich Plasma Carrying Icariin Enhances Bone-Tendon Healing in a Rabbit Model. Am J Sports Med, 2019; 47: 1964-74.
27. Zhang M, J Zhen, X Zhang, Z Yang, L Zhang, D Hao, et al:. Effect of Autologous Platelet-Rich Plasma and Gelatin Sponge for Tendon-to-Bone Healing After Rabbit Anterior Cruciate Ligament Reconstruction. Arthroscopy, 2019; 35: 1486-97.
28. Shen H, H Lin, AX Sun, S Song, B Wang, Y Yang, et al:. Acceleration of chondrogenic differentiation of human mesenchymal stem cells by sustained growth factor release in 3D graphene oxide incorporated hydrogels. Acta Biomater, 2020; 105: 44-55.
29. Qi C, Y Deng, L Xu, C Yang, Y Zhu, G Wang, et al:. A sericin/ graphene oxide composite scaffold as a biomimetic extracellular matrix for structural and functional repair of calvarial bone. Theranostics, 2020; 10: 741-56.
30. Kwon J, YH Kim, SM Rhee, TI Kim, J Lee, S Jeon, et al:. Effects of Allogenic Dermal Fibroblasts on Rotator Cuff Healing in a Rabbit Model of Chronic Tear. Am J Sports Med, 2018; 46: 1901-08.
31. Beck J, D Evans, PM Tonino, S Yong, JJ Callaci. The biomechanical and histologic effects of platelet-rich plasma on rat rotator cuff repairs. Am J Sports Med, 2012; 40: 2037-44.
32. Chung SW, BW Song, YH Kim, KU Park, JH Oh. Effect of platelet-rich plasma and porcine dermal collagen graft augmentation for rotator cuff healing in a rabbit model. Am J Sports Med, 2013; 41: 2909-18.
33. Lamplot JD, M Angeline, J Angeles, M Beederman, E Wagner, F Rastegar, et al:. Distinct effects of platelet-rich plasma and BMP13 on rotator cuff tendon injury healing in a rat model. Am J Sports Med, 2014; 42: 2877-87.
34. Randelli P, P Arrigoni, V Ragone, A Aliprandi, P Cabitza. Platelet rich plasma in arthroscopic rotator cuff repair: a prospective RCT study, 2-year follow-up. J Shoulder Elbow Surg, 2011; 20: 518-28.

35. Rodeo SA, D Delos, RJ Williams, RS Adler, A Pearle, RF Warren. The effect of platelet-rich fibrin matrix on rotator cuff tendon healing: a prospective, randomized clinical study. Am J Sports Med, 2012; 40: 1234-41.
36. Gugjoo MB, GT Sharma, HP Aithal, P Kinjavdekar. Cartilage tissue engineering: Role of mesenchymal stem cells along with growth factors & scaffolds. Indian J Med Res, 2016; 144: 339-47.
37. Zhou M, N Lozano, JK Wychowaniec, T Hodgkinson, SM Richardson, K Kostarelos, et al:. Graphene oxide: A growth factor delivery carrier to enhance chondrogenic differentiation of human mesenchymal stem cells in 3D hydrogels. Acta Biomater, 2019; 96: 271-80.
38. Suh DS, JK Lee, JC Yoo, SH Woo, GR Kim, JW Kim, et al:. Atelocollagen Enhances the Healing of Rotator Cuff Tendon in Rabbit Model. Am J Sports Med, 2017; 45: 2019-27.

Figures

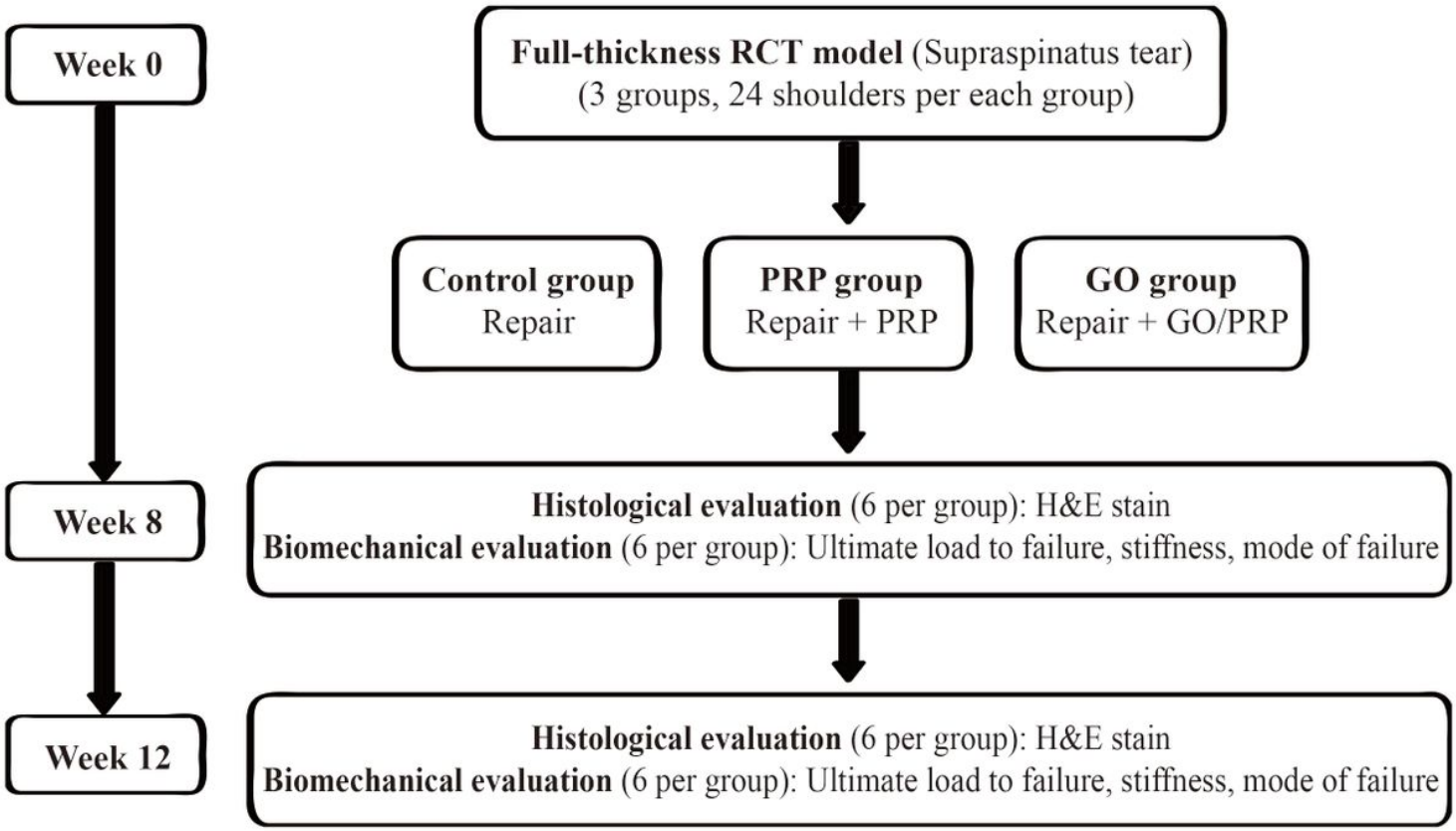

Figure 1

The study flowchart.

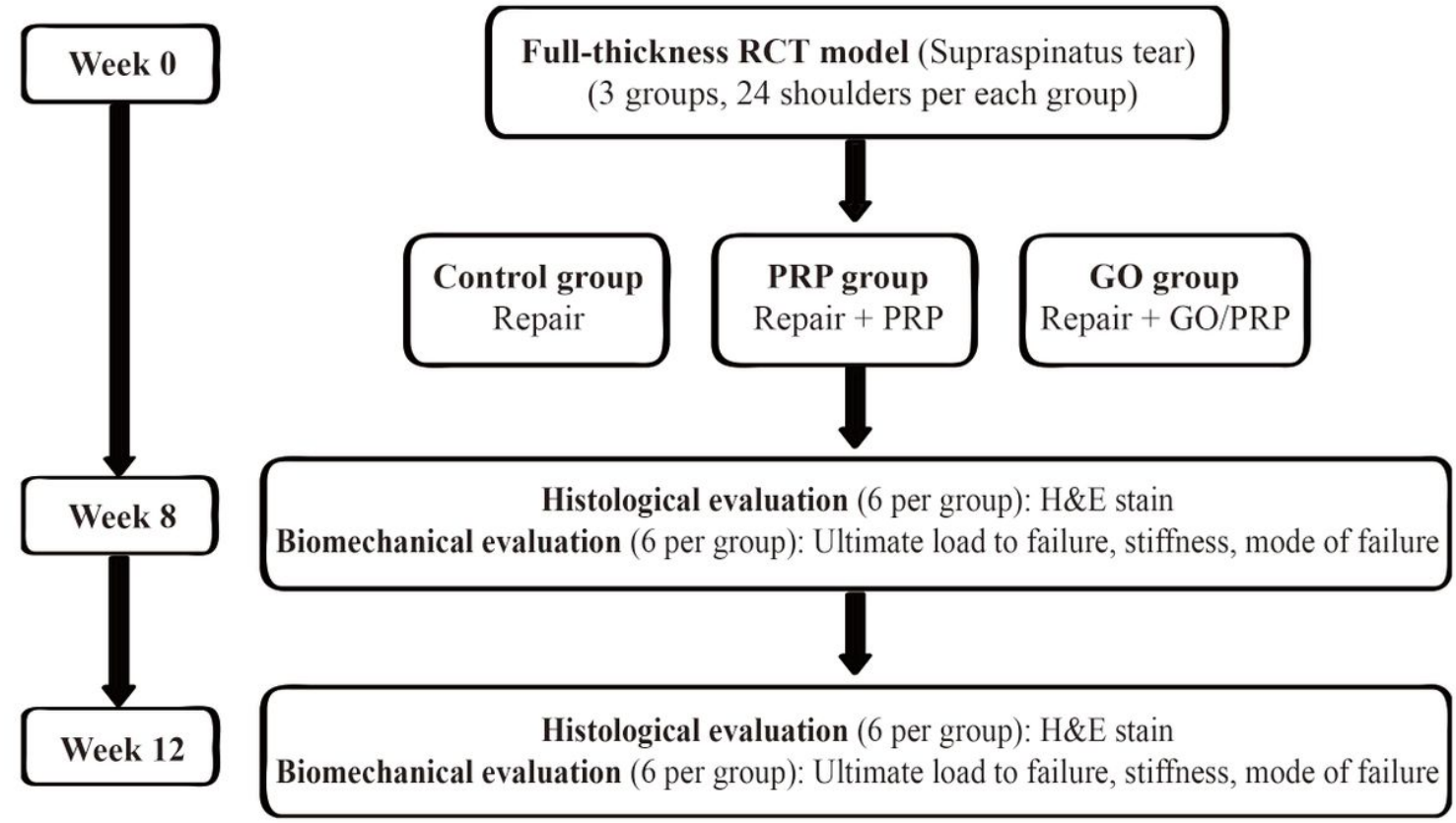

Figure 1

The study flowchart.

Figure 2

The preparation of acute full-thickness RCT model. A, exploration of the supraspinatus tendon. B, full-thickness RCT model was created, and the torn tendon was sutured by transosseous fixation. C, the illustration of transosseous fixation was shown.

Figure 2

The preparation of acute full-thickness RCT model. A, exploration of the supraspinatus tendon. B, full-thickness RCT model was created, and the torn tendon was sutured by transosseous fixation. C, the illustration of transosseous fixation was shown.

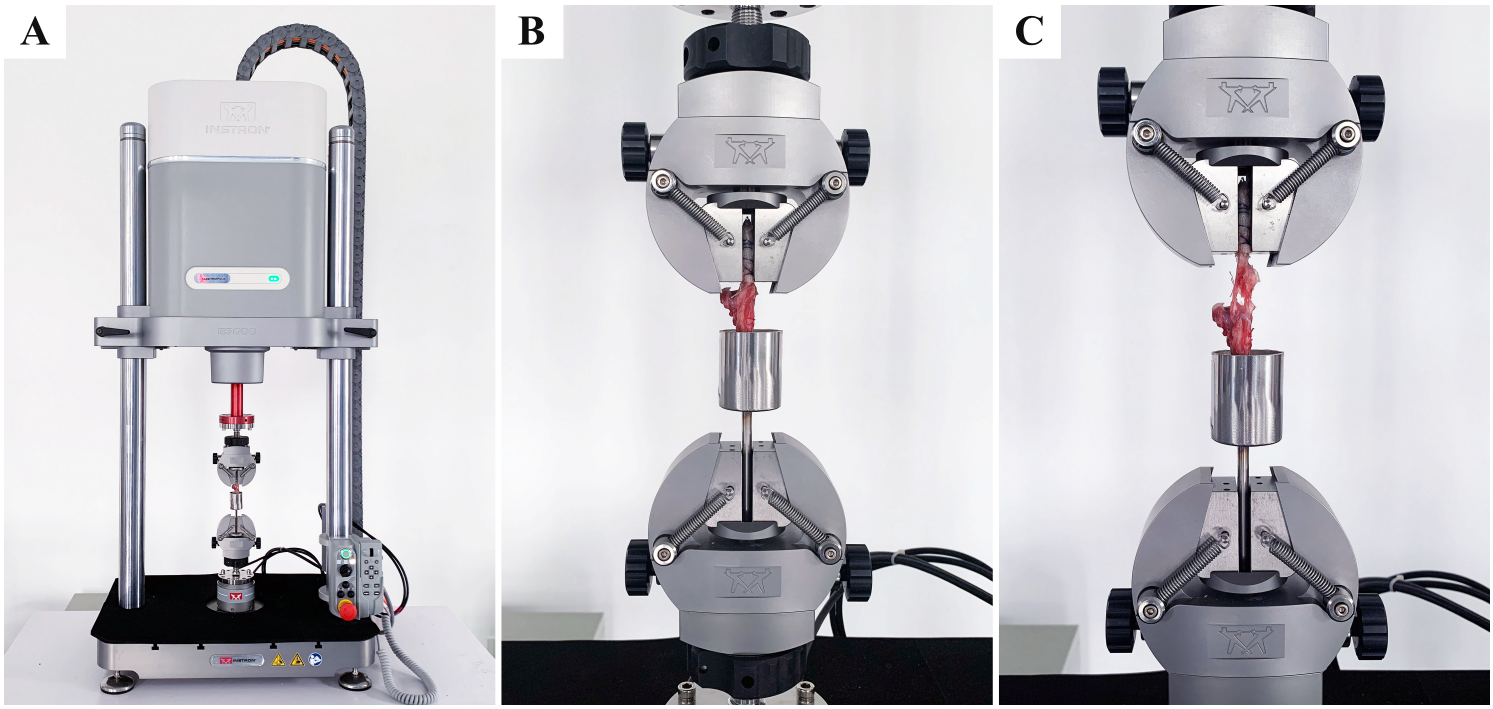

Figure 3

The diagram of biomechanical evaluation. A, panorama. The tendon-bone complex was firmly fixed on the INSTRON machine to perform the biomechanical test. B, detail view. The machine with a custom fixture clamping system is shown. C, the tendon-bone complex was loaded until it pulled apart from the bone (TBI) or ruptured at the tendinous part.

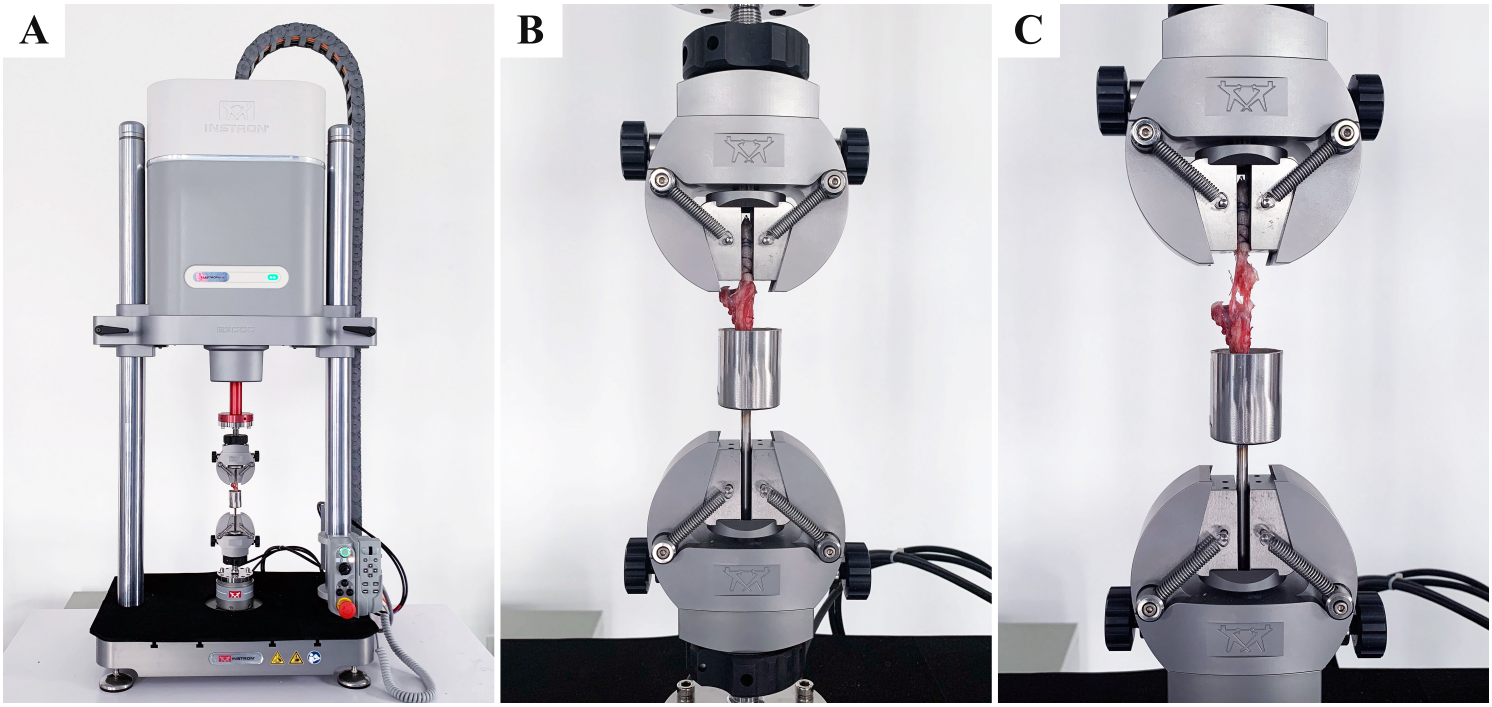

Figure 3

The diagram of biomechanical evaluation. A, panorama. The tendon-bone complex was firmly fixed on the INSTRON machine to perform the biomechanical test. B, detail view. The machine with a custom fixture clamping system is shown. C, the tendon-bone complex was loaded until it pulled apart from the bone (TBI) or ruptured at the tendinous part.

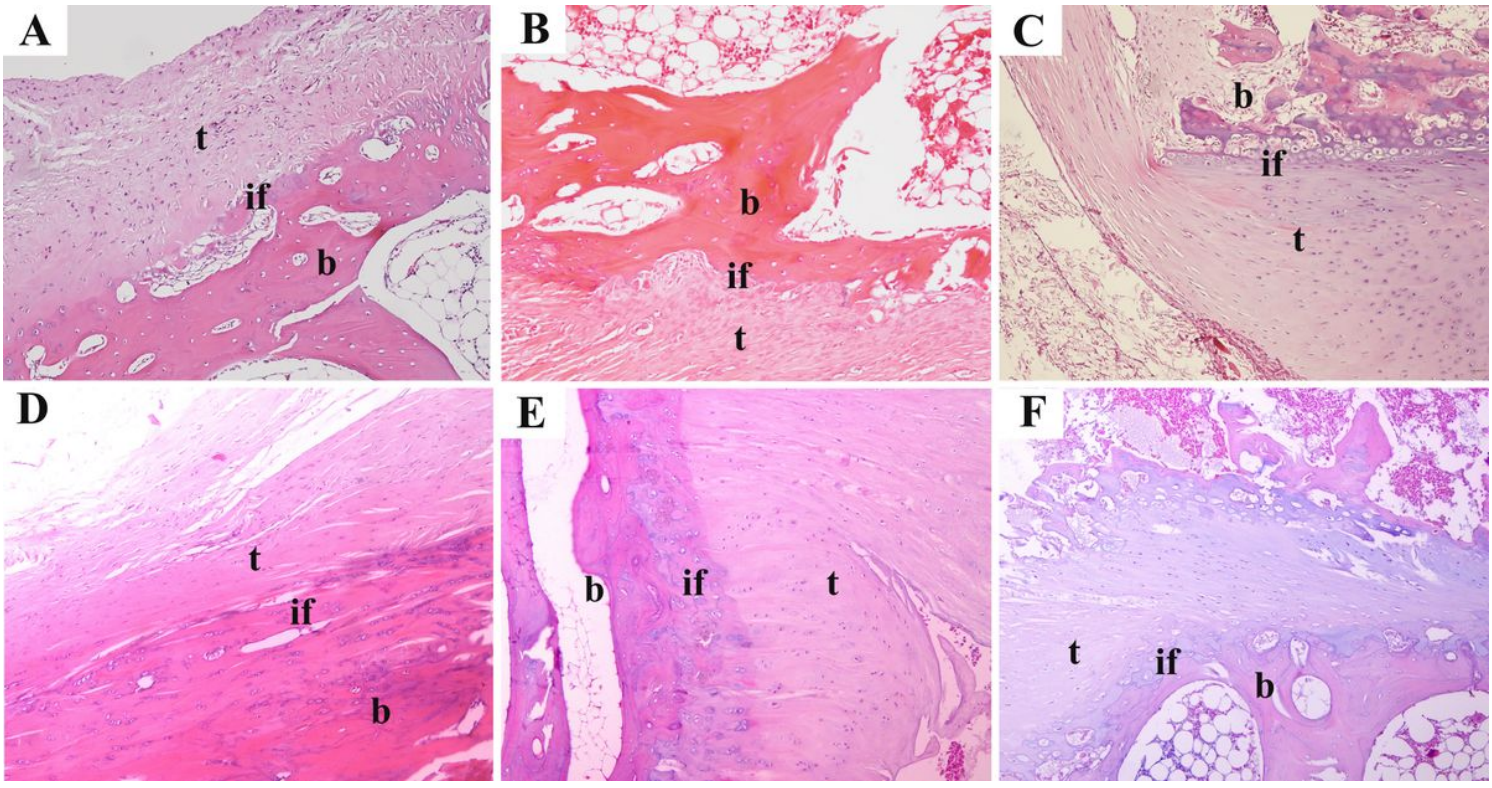

Figure 4

Histological evaluation of representative HE-stained images at 8 and 12 weeks after surgery (×100). At 8 weeks: A, Control group; B, PRP group; C, GO group. At 12 weeks: D, Control group; E, PRP group; F, GO group.

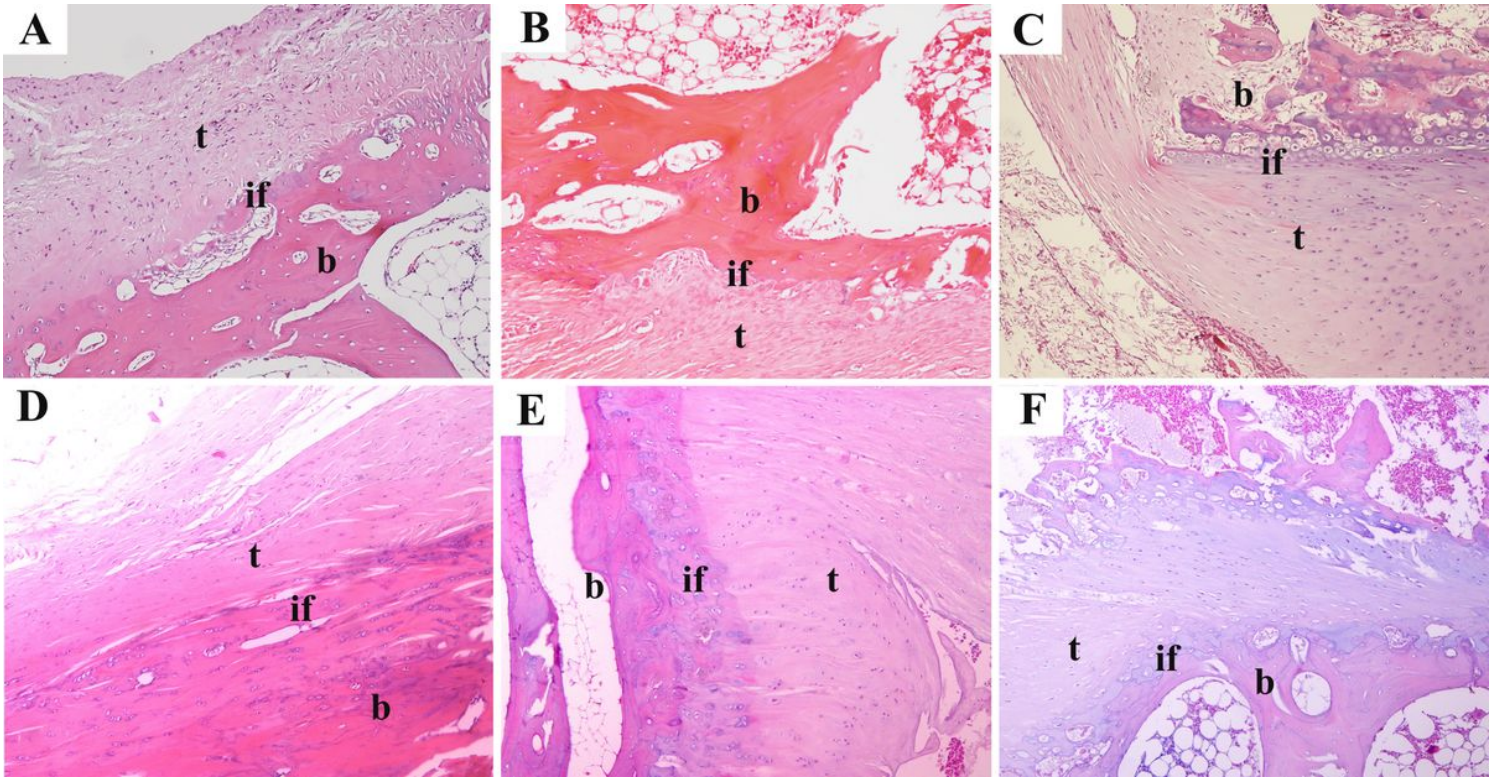

Figure 4

Histological evaluation of representative HE-stained images at 8 and 12 weeks after surgery (×100). At 8 weeks: A, Control group; B, PRP group; C, GO group. At 12 weeks: D, Control group; E, PRP group; F, GO group.

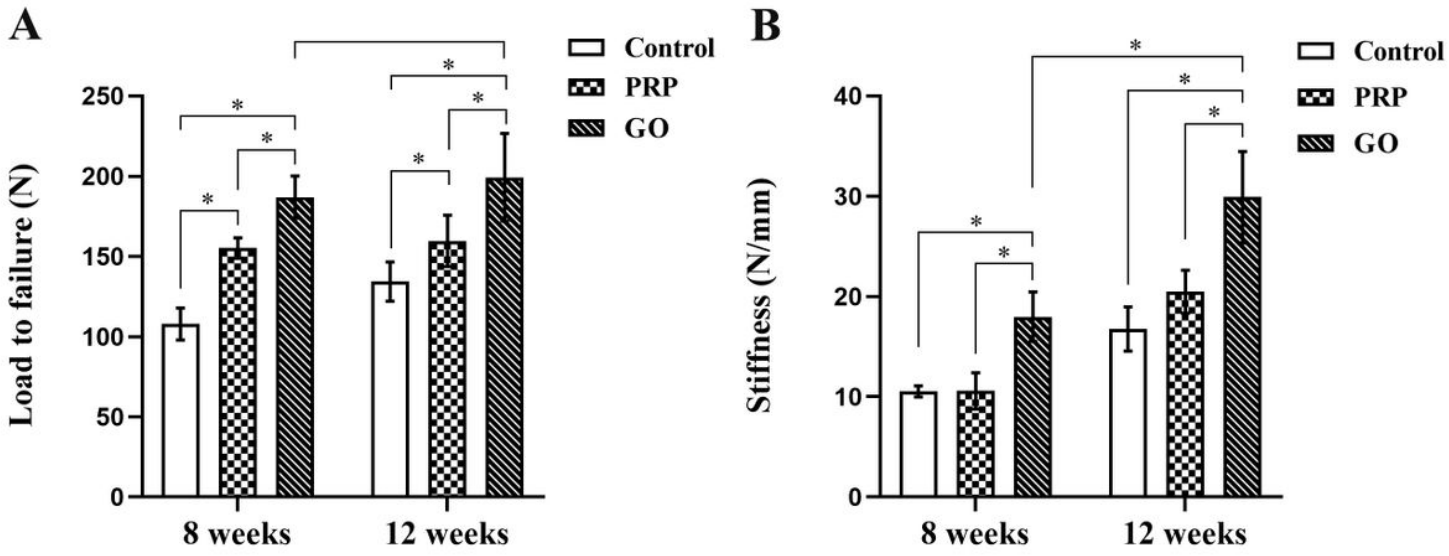

Figure 5

Biomechanical evaluation at 8 and 12 weeks after surgery. GO group showed a higher load significantly to failure and stiffness than the other groups. A, the load to failure of three groups was determined. B, the stiffness of the three groups was determined. The asterisk (*) designates a significant difference between two groups (P<0.05).

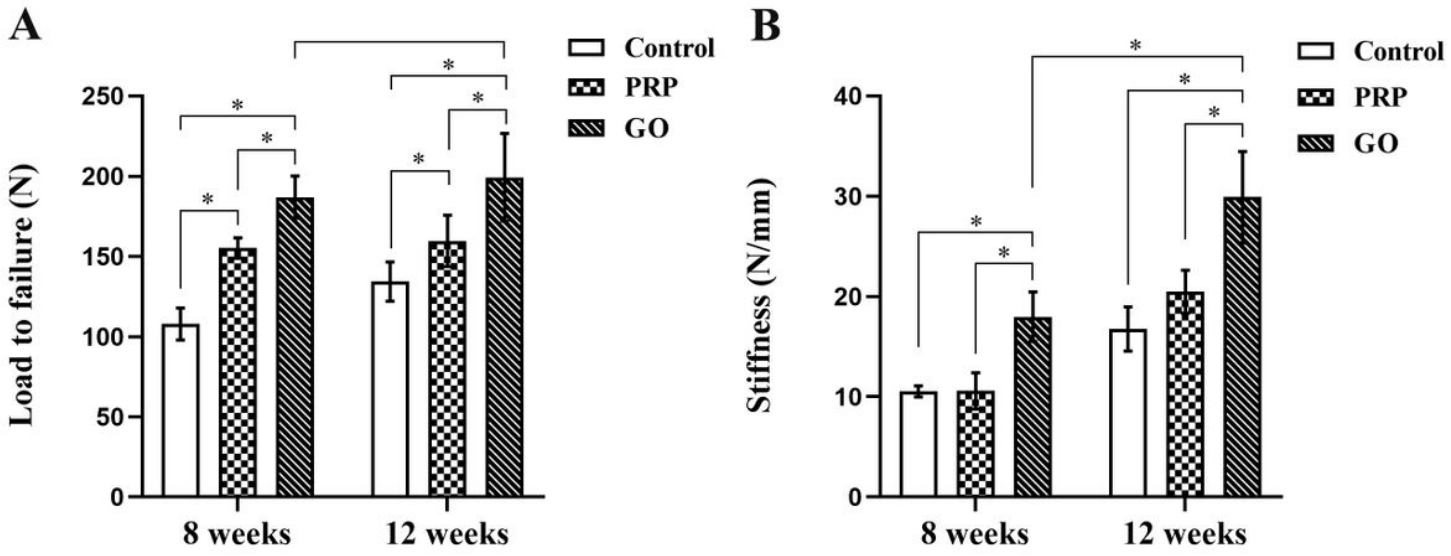

Figure 5

Biomechanical evaluation at 8 and 12 weeks after surgery. GO group showed a higher load significantly to failure and stiffness than the other groups. A, the load to failure of three groups was determined. B, the stiffness of the three groups was determined. The asterisk (*) designates a significant difference between two groups (P<0.05).

Supplementary Files

This is a list of supplementary files associated with this preprint. Click to download.

- Biomechanicalevaluations.pdf
- Biomechanicalevaluations.pdf
- Histologicalevaluations.pdf
- Histologicalevaluations.pdf